



OPEN Prognostic impact of extracellular volume fraction derived from equilibrium contrast-enhanced CT in HCC patients receiving immune checkpoint inhibitors

Xiaona Fu^{1,2,3}, Yusheng Guo^{1,2,3}, Kailu Zhang^{1,2,3}, Zhixuan Cheng^{1,2}, Chanyuan Liu^{1,2}, Yi Ren^{1,2}, Lianwei Miao^{1,2}, Weiwei Liu^{1,2}, Shanshan Jiang^{1,2}, Chen Zhou^{1,2}✉, Yangbo Su^{1,2}✉ & Lian Yang^{1,2}✉

This study aimed to investigate whether extracellular volume (ECV) fraction derived from equilibration contrast-enhanced computed tomography (CECT) affects prognosis in HCC patients receiving ICIs. This retrospective study ultimately included 211 HCC patients undergoing ICIs, of whom 60 were included in an internal validation to assess the reproducibility of the results. Baseline unenhanced and equilibrated CECT were used to measure CT values of the tumor, liver and aorta, which were combined with hematocrit to calculate the ECV fraction. Correlation analysis was used to investigate the association between tumor ECV and liver ECV fractions. The effects of clinical variables and ECV fraction on progression-free survival (PFS) and overall survival (OS) were evaluated using Cox proportional hazards models and Kaplan-Meier curves. Of these 151 patients, tumor ECV fraction positively correlated with liver ECV fraction. In the Lower tumor ECV group, PFS (5.6 vs. 7.6 months) and OS (10.5 vs. 15.5 months) were notably shorter than in the Higher tumor ECV group, while no significant differences were found between the Higher and Lower liver ECV groups. Furthermore, the multivariable Cox regression model demonstrated that higher tumor ECV fraction level was an independent protective factor for PFS and OS (all $P < 0.001$). Internal validation cohort preliminary demonstrated reproducibility of results. The tumor ECV fraction is expected to become a routine indicator before ICIs therapy for HCC patients in contrast to liver ECV fraction, contributing to their subsequent management.

Keywords Extracellular volume fraction, Immune checkpoint inhibitors, Hepatocellular carcinoma, Prognosis

Abbreviations

ICIs	Immune checkpoint inhibitors
HCC	Hepatocellular carcinoma
ECV	Extracellular volume
CECT	Contrast-enhanced computed tomography
CR	Complete response
PR	Partial response
SD	Stable disease
PD	Disease progression
ORR	Objective remission rate
DCR	Disease control rate
PFS	Progression-free survival

¹Department of Radiology, Union Hospital, Tongji Medical College, Huazhong University of Science and Technology, Wuhan 430022, China. ²Hubei Key Laboratory of Molecular Imaging, Wuhan 430022, China. ³These authors contributed equally to this work: Xiaona Fu, Yusheng Guo and Kailu Zhang. ✉email: zhouchenjr@126.com; suyangbough@sina.com; yanglian@hust.edu.cn

OS	Overall survival
PDAC	Pancreatic ductal adenocarcinoma
BMI	Body mass index
HBV	Hepatitis B virus
ICIs	Immune checkpoint inhibitors
TKIs	Tyrosine kinase inhibitors
PVTT	Portal vein tumor thrombosis
BCLC	Barcelona Clinic Liver Cancer
ECOG PS	Eastern Cooperative Oncology Group Physical Status
NLR	Neutrophil to lymphocyte ratio
PLR	Platelet to lymphocyte ratio
ALT	Alanine transaminase, AST, Aspartate transaminase
TB	Total bilirubin
PT	Prothrombin time
AFP	Alpha-fetoprotein. ROIs, regions of interest
ICC	Intraclass correlation coefficients
CI	Confidence interval

Liver cancer is one of the most widespread cancers globally. Its incidence has been steadily increasing in Western countries in recent years, but still 72% of new cases globally are diagnosed in Asia¹. Hepatocellular carcinoma (HCC) has the highest prevalence of primary liver cancer and ranks third in cancer-related deaths globally^{2–4}. Recently immune checkpoint inhibitors (ICIs) therapy, comprising anti-programmed cell death protein 1 (PD-1), anti-programmed death-ligand 1(PD-L1), and anti-cytotoxic T-lymphocyte-associated protein 4 (CTLA-4), have provided significant clinical benefits for advanced tumors such as HCC^{5–7}. However, and several HCC patients develop primary or secondary resistance to anti-immunotherapy during treatment⁸. Therefore, reliable predictive markers are urgently needed to identify HCC patients suitable for ICIs therapy.

Contrast-enhanced computed tomography (CECT) is of great diagnostic value in the diagnosis of hepatocellular carcinoma, as it enables to show the tumor location, size and other characteristics⁹. Extracellular volume (ECV) is a significant biological concept attracting widespread attention. ECV is the total of the extracellular-extravascular and intravascular spaces to quantify the extracellular matrix, a non-cellular component present in all tissues and organs of the body, reflecting the extent of tumor vascular infiltration, stromal fibrosis, and the tumor microenvironment¹⁰. And it is more objective with correction for hematocrit. Currently, studies have shown that the tumor microenvironment is a crucial mediator of cancer progression and treatment outcome¹¹, and tumor ECV fraction measured based on CT or MR have been progressively used for differential diagnosis of tumors, degree of differentiation, prognosis, and efficacy assessment^{12–14}. Takumi et al. revealed that the tumor ECV fraction obtained from CECT aids in the diagnosis of anterior mediastinal tumors¹⁵. Fukukura et al. investigated that tumor ECV fraction measured using equilibrium CECT imaging had the potential to serve as a prognostic indicator for survival outcomes in patients with stage IV pancreatic ductal adenocarcinoma (PDAC) undergoing chemotherapy¹⁶. In addition, tumor ECV fraction derived from equilibrium CECT could predict the complete pathological response of locally advanced rectal cancer after neoadjuvant radiotherapy and chemotherapy¹⁷.

With regards to studies in the liver, tumor ECV fraction has been used to predict pathologic grading of HCC and liver ECV fraction to assess the severity of liver fibrosis and cirrhosis^{18,19}, but studies of ECV fraction based on CECT as an imaging marker for predicting survival of HCC patients receiving ICIs therapy have not been reported. Therefore, to explore the clinical application of equilibrium CECT-ECV in the survival outcomes of HCC patients receiving ICIs therapy, we retrospectively analyzed the status of these patients and followed them up.

Materials and methods

Patients

The research project was granted approval by the local ethics committee and institutional review board, and its methodology aligns with the standards in the Strengthening the reporting of observational studies in epidemiology (STROBE)²⁰. All methods were performed in accordance with the relevant guidelines and regulations. In light of the retrospective nature of this study, the necessity for obtaining informed consent from the participants was waived. This study ultimately included 211 HCC patients treated with ICIs at the Union Hospital of Tongji Medical College in China between July 2020 and December 2023, with data from 60 patients from other branches used for internal validation. Inclusion and exclusion criteria as follows: (1) diagnosis of HCC according to European Association for the Study of Liver (EASL)²¹, (2) Child-Pugh A or B; (2) age > 18 years, (3) receiving at least two cycles of immunotherapy and (4) liver enhancement CT performed before initial ICIs therapy with less than 1 week interval from hematocrit for calculation of ECV fraction. Exclusion criteria: (1) combination with other primary tumors; (2) patients treated with surgical resection prior to ICIs therapy, (3) Child-Pugh C; (4) patients with incomplete medical records at the start of ICIs therapy and during follow-up; and (5) incomplete clinical and imaging data. All baseline data were obtained from patients' electronic medical records and included the following variables: age, sex, body mass index (BMI), history of hepatitis and HBV, types of ICIs, combined with tyrosine kinase inhibitors (TKIs), Child-Pugh classification, Barcelona Clinic Liver Cancer (BCLC) stage, Eastern Cooperative Oncology Group Physical Status (ECOG-PS), portal vein tumor thrombosis (PVTT), and laboratory indicators.

CT imaging strategy

All patients signed an informed consent form before undergoing abdominal CECT. Before scanning, patients were required to fast for 8 h and underwent iodine allergy testing. All patients underwent liver scanning on a 128-row CT scanner (SIEMENS SOMATOM Definition AS+, Siemens Healthcare Erlangen, Germany) using the following parameters: tube voltage 120 kV, tube current using automatic milliamp technology, both layer thickness and layer spacing 1.5 mm, and matrix 512 × 512. Patients were placed in the supine position during the scanning process. Contrast was injected into the elbow vein (concentration 350 mg/ml, flow rate 2–3 ml/s). Enhanced images were acquired at different time points after contrast injection: 25–30 s for the arterial phase, 50–60 s for the portal venous phase, and 120–180 s for the equilibrium phase.

Extracellular volume fraction analysis

Two radiologists (with 5 and 10 years' experience in abdominal radiology, respectively) analyzed the images on the Picture Archiving and Communication System (PACS), unaware of patient clinical data but knowing the location of the largest HCC. Tumor attenuation values were measured at the level of the maximum diameter of the HCC on unenhanced and equilibrium CECT images of all patients. Place circular or oval regions of interest (ROIs) within the HCC as large as possible avoiding necrosis and hemorrhage. For multiple lesions, we placed the ROIs at the largest representative lesion with the largest diameter for CT value measurement. Meanwhile, two radiologists manually placed three liver ROIs on the images (each approximately 100 mm²), excluding large intrahepatic vessels and liver tumors. The ROIs were located in the anterior and posterior segments of the right lobe as well as the left lateral segment, with their average taken as the liver CT value. Within the abdominal aorta at the same level, the ROIs were placed in the same location in each patient in both unenhanced and equilibrium CECT, avoiding vessel wall calcifications and wall thrombus (approximately 100 mm²) (Fig. 1). Region of interest CT values measured by two radiologists were averaged, and disagreements were resolved by consensus. The ECV fraction of HCC lesions was determined by the equation: tumor ECV (%) = (1 - hematocrit) × (ΔHU_{tumor} / ΔHU_{tumor-aorta}) × 100%. The formula for liver ECV fraction was liver ECV (%) = (1 - hematocrit) × (ΔHU_{liver} / ΔHU_{liver-aorta}) × 100%. ΔHU_{tumor}, ΔHU_{liver}, ΔHU_{tumor-aorta} and ΔHU_{liver-aorta} represent HU in the equilibrium CECT minus unenhanced for tumor, liver and aorta (tumor or liver parenchyma plane), respectively.

Follow-up

Patients' follow-up data were obtained through electronic medical records, imaging data, and telephone communication. They were followed up until May 2024. In accordance with the Modified Response Evaluation Criteria in Solid Tumors (mRECIST)²², tumor remission was classified as complete response (CR), partial response (PR), stable disease (SD), or disease progression (PD). The objective remission rate (ORR) was determined as the sum of CR and PR, while the disease control rate (DCR) was calculated by adding the CR, PR, and SD. Progression-free survival (PFS) was determined to be the interval between the initial immunotherapy treatment and the occurrence of tumor progression or patient demise. Overall survival (OS) was defined similarly, but with the initial immunotherapy treatment marking the starting point and the last follow-up or patient death marking the endpoint.

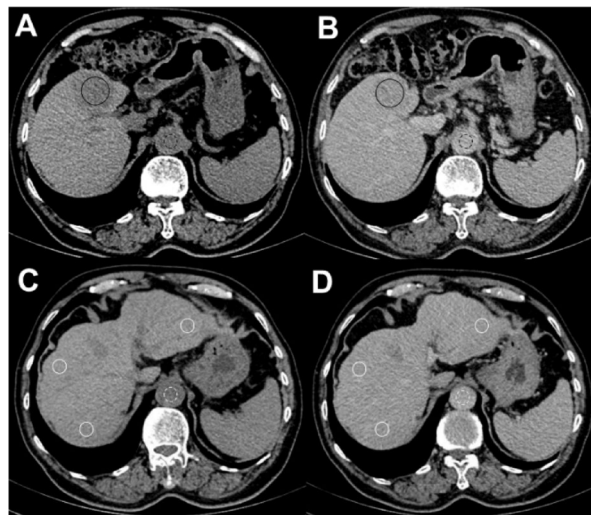


Fig. 1. ECV fraction position of a 79 years old male with hepatocellular carcinoma receiving immune checkpoint inhibitors. Axial unenhanced (A) and equilibration contrast-enhanced CT (B) show ROIs on the 4.5 centimeters tumor (black circle) and aorta (black dashed circle). Axial unenhanced (C) and equilibration contrast-enhanced CT (D) show ROIs on the anterior and posterior segments of the right lobe and lateral segment of the left lobe of the liver (white circle) and the aorta (white dashed circle). The tumor ECV fraction was 38.48%, liver ECV fraction was 28.07%.

Statistical analysis

Continuous variables are indicated by mean (SD) or median (IQR), which were subsequently compared using t-test or Wilcoxon rank-sum test. Categorical variables are indicated by counts (percentages) and were compared using chi-square test. Interobserver agreement of CT values in the tumors, liver and aorta was assessed using intraclass correlation coefficients (ICC). Exploring the association between tumor ECV fraction and liver ECV fraction using Spearman's rank correlation analysis X-tile software (<https://medicine.yale.edu/lab/rimm/research/software/>), which provides a comprehensive method for dividing cohorts into low and high levels of marker expression based on survival curves, was used to determine cut-off values for the ECV fraction. The Kaplan-Meier curve and log-rank test were employed to ascertain disparities in PFS and OS between two groups. Variables with $P < 0.1$ in univariate analysis were included in the multivariate Cox regression model in the Cox regression analysis. Forest plots showed unstratified univariate Cox models calculating hazard ratios of PFS and OS for each subgroup. With all tests being two-tailed, $P < 0.05$ was considered statistically significant. All analyses within this study were performed using SPSS software (version 25.0, SPSS Inc., Chicago, IL, USA) and R version 4.3.0 (R Foundation).

Results

Patient demographics and clinical characteristics

A total of 151 patients with HCC treated with ICIs (including 62 Lower tumor ECV and 89 tumor Higher ECV, or 73 Lower liver ECV and 78 Higher Liver ECV) were ultimately included in the present study. Table 1 showed the basic demographic and clinical characteristics in both tumor ECV groups. No significant differences in age, sex and BMI were observed within the two groups. There were more males than females in both groups, which was consistent with the epidemiology of higher prevalence of HCC in males compared to females. Although there were no significant differences in history of HBV infection between the two groups, the Higher tumor ECV group had a higher proportion of people without HBV infection (62.9% vs. 51.6%) than the Lower tumor ECV group. In addition, no statistically significant differences were found between the two groups in biochemical indicators such as neutrophil to lymphocyte ratio (NLR), platelet to lymphocyte ratio (PLR), alpha-fetoprotein (AFP), etc. Baseline characteristics of patients with low liver ECV and high liver ECV were also shown in Supplementary Table 1.

The correlation analysis and optimum cutoff value of ECV fraction

Tumor ECV fraction showed a significant positive correlation with liver ECV fraction ($\rho = 0.203$, $P = 0.012$, Fig. 2). Meanwhile, the CT values of tumor and aorta on same plane in the unenhanced (tumor, ICC = 0.91; 95% CI, 0.88–0.94; aorta, ICC = 0.91; 95% CI, 0.87–0.93) and equilibrium (tumor, ICC = 0.97; 95% CI, 0.96–0.98; aorta, ICC = 0.98; 95% CI, 0.97–0.98) had excellent interobserver agreement. For ECV fraction of liver parenchyma, CT values of liver parenchyma and aorta on same plane in the unenhanced (liver, ICC = 0.96; 95% CI, 0.95–0.97; aorta, ICC = 0.90; 95% CI, 0.86–0.93) and equilibrium (liver, ICC = 0.99; 95% CI, 0.98–0.99; aorta, ICC = 0.99; 95% CI, 0.98–0.99) also had excellent interobserver agreement. The X-tile software was utilized to ascertain thresholds for classification of the tumor ECV and liver ECV fractions (Supplementary Fig. 1). The OS time of the enrolled patients served as a point of reference. By ensuring that the OS trends of both patient groups were consistent across all cutoff points, we identified the point where the difference in outcomes between the two groups was most significant. The optimal cutoff value for tumor ECV fraction in this study was 27.2, and 62 patients were finally included in Lower ECV group and 89 in Higher ECV group. The best cutoff for liver ECV fraction was 29.0, which included 73 patients in Lower liver ECV group and 78 patients in Higher liver ECV group.

Tumor response

Tumor responses of tumor ECV groups and liver ECV groups were shown in Supplementary Tables 2 and Supplementary Table 3. According to mRECIST criteria, short-term treatment outcomes were similar between the tumor ECV groups, with no statistically significant differences between the Lower tumor ECV and Higher tumor ECV groups in terms of DCR (62.9% vs. 75.3%, $P = 0.102$) and ORR (25.8% vs. 34.8%, $P = 0.239$). Similarly, there were no significant differences in ORR (35.6% vs. 26.9%, $P = 0.239$) and DCR (74% vs. 66.7%, $P = 0.327$) between the Lower liver ECV group and Higher liver ECV group.

Survival analysis

A total of 83 patients had died by the time of analysis, including 35 patients in the Lower tumor ECV group and 48 in the Higher tumor ECV group. In this study, The median PFS of 6.4 months (95% CI [5.7–8.5]) and a median survival time of 12.9 months (95% CI [12.3–15.8]) in all patients. Kaplan-Meier curves for PFS and OS were analyzed for tumor ECV and liver ECV groups. The log-rank test showed that PFS (5.6 vs. 7.6 months, $P < 0.001$) and OS (10.5 vs. 15.5 months, $P < 0.001$) were shorter in the Lower tumor ECV group than in the Higher tumor ECV group (Fig. 3). However, there were no significant differences in PFS (6.9 vs. 6 months, $P = 0.346$) and OS (12.6 vs. 13.1 months, $P = 0.729$) between the Lower liver ECV and Higher liver ECV groups (Supplementary Fig. 2). Meanwhile, Fig. 4 demonstrated the heatmap of the relationship between tumor, liver ECV fraction and clinical characteristics with OS for each patient.

Univariate and multivariate Cox regression analyses

In univariate regression analysis, age, tumor maximum diameter, PVTT, BCLC stage, NLR, PLR and tumor ECV group were identified as potential predictors for PFS. Sex, tumor maximum diameter, PVTT, BCLC stage, NLR, AFP level and tumor ECV group were for potential predictors of OS. These variables were further incorporated into multivariate regression analysis. In multivariate analysis, BCLC-C stage was independent risk

Characteristics	Total population (n = 151)	Lower tumor ECV (n = 62)	Higher tumor ECV (n = 89)	P value
Age (years), n (%)				0.085
< 60	88 (58.3%)	31 (50%)	57 (64%)	
≥ 60	63 (41.7%)	31 (50%)	32 (36%)	
Sex, n (%)				0.155
Female	22 (14.6%)	6 (9.7%)	16 (18%)	
Male	129 (85.4%)	56 (90.3%)	73 (82%)	
BMI (kg/m ²), mean (SD)	23 (3.1)	22.7 (3.2)	23.1 (3.1)	0.418
HBV infection, n (%)				0.166
No	88 (58.3%)	32 (51.6%)	56 (62.9%)	
Yes	63 (41.7%)	30 (48.4%)	33 (37.1%)	
Types of ICIs, n (%)				1.000
PD-1	141 (93.4%)	58 (93.5%)	83 (93.3%)	
PD-L1	10 (6.6%)	4 (6.5%)	6 (6.7%)	
Combined with TKIs, n (%)				0.332
No	68 (45%)	25 (40.3%)	43 (48.3%)	
Yes	83 (55%)	37 (59.7%)	46 (51.7%)	
Tumor maximum diameter (cm), median (IQR)	6.6 (3.7, 10.5)	7.9 (4.2, 11.5)	6.6 (3.5, 10.2)	0.341
Tumor number, n (%)				0.906
≤ 3	126 (83.4%)	52 (83.9%)	74 (83.1%)	
> 3	25 (16.6%)	10 (16.1%)	15 (16.9%)	
PVTT, n (%)				0.239
No	110 (72.8%)	42 (67.7%)	68 (76.4%)	
Yes	41 (27.2%)	20 (32.3%)	21 (23.6%)	
Lymph node metastasis, n (%)				0.805
No	116 (76.8%)	47 (75.8%)	69 (77.5%)	
Yes	35 (23.2%)	15 (24.2%)	20 (22.5%)	
BCLC stage, n (%)				0.218
B	65 (43%)	23 (37.1%)	42 (47.2%)	
C	86 (57%)	39 (62.9%)	47 (52.8%)	
Child-Pugh, n (%)				0.608
A	134 (88.7%)	56 (90.3%)	78 (87.6%)	
B	17 (11.3%)	6 (9.7%)	11 (12.4%)	
ECOG PS, n (%)				0.101
0	115 (76.2%)	43 (69.4%)	72 (80.9%)	
≥ 1	36 (23.8%)	19 (30.6%)	17 (19.1%)	
NLR, median (IQR)	2.4 (1.7, 3.5)	2.3 (1.6, 3.5)	2.6 (1.8, 3.3)	0.409
PLR, median (IQR)	121.3 (93.2, 161)	118.5 (84.1, 158.8)	125 (97.6, 161.2)	0.401
ALT (U/L), median (IQR)	34 (23, 54)	33.5 (26, 47.5)	34 (22, 56)	0.914
AST (U/L), median (IQR)	44 (32, 70)	49 (33, 76.8)	44 (32, 64)	0.563
TB (μmol/L), median (IQR)	15.4 (11.2, 20.7)	16 (11.3, 21.4)	14.7 (11.1, 20.4)	0.379
Albumin (g/L), median (IQR)	36.5 (32.8, 40.2)	37.6 (32.8, 40.3)	36.3 (32.9, 39.8)	0.840
PT (s), median (IQR)	13.6 (13.1, 14.4)	13.9 (13.2, 14.6)	13.5 (13.1, 14.3)	0.139
Creatinine (μmol/L), median (IQR)	67.3 (57.6, 76.2)	70.5 (61.3, 76.5)	64.7 (56.6, 75)	0.103
Urea nitrogen (mmol/L), median (IQR)	4.67 (3.8, 5.9)	4.6 (3.9, 5.8)	4.8 (3.6, 5.9)	0.800
AFP (ng/mL), n (%)				0.886
< 400	96 (63.6%)	39 (62.9%)	57 (64%)	
≥ 400	55 (36.4%)	23 (37.1%)	32 (36%)	

Table 1. Baseline characteristics of patients. *ECV* extracellular volume, *BMI* body mass index, *HBV* hepatitis B virus, *ICIs* immune checkpoint inhibitors, *TKIs* tyrosine kinase inhibitors, *PVTT* portal vein tumor thrombosis, *BCLC* Barcelona clinic liver cancer, *ECOG PS* eastern cooperative oncology group physical status, *NLR* neutrophil to lymphocyte ratio, *PLR* platelet to lymphocyte ratio, *ALT* alanine transaminase, *AST* aspartate transaminase, *TB* total bilirubin, *PT* prothrombin time, *AFP* alpha-fetoprotein.

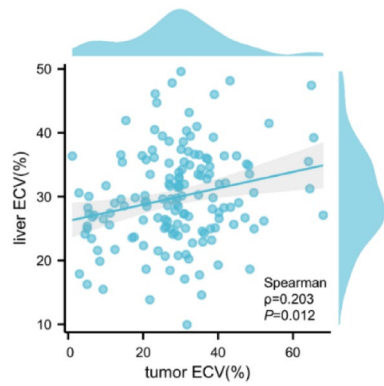


Fig. 2. Correlation analysis of tumor ECV fraction with liver ECV fraction.

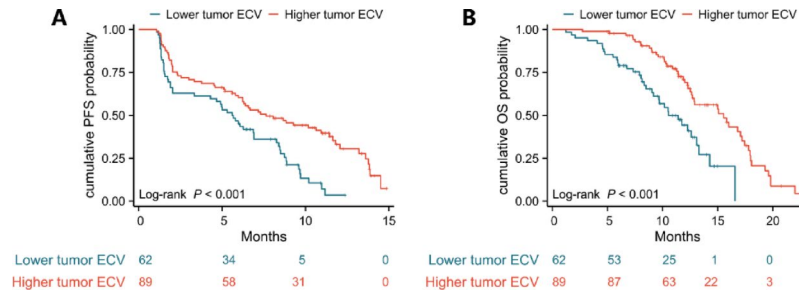


Fig. 3. Kaplan-Meier curves of PFS (A) and OS (B) for Lower tumor ECV group (blue) and Higher tumor ECV group (red). PFS progression-free survival, OS overall survival, ECV extracellular volume.

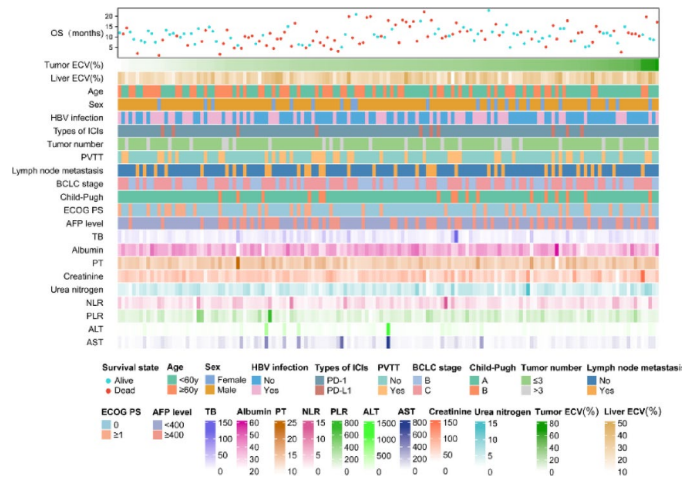


Fig. 4. Heatmap showed the relationship between tumor, liver ECV fraction and clinical characteristics with OS for each patient. ECV extracellular volume, HBV hepatitis B virus, ICIs immune checkpoint inhibitors, PVT portal vein tumor thrombosis, BCLC Barcelona clinic liver cancer, ECOG PS eastern cooperative oncology group physical status, NLR neutrophil to lymphocyte ratio, PLR platelet to lymphocyte ratio, ALT alanine transaminase, AST aspartate transaminase, TB total bilirubin, PT prothrombin time, AFP alpha-fetoprotein.

factor for shorter PFS (HR, 1.69 [95%CI, 1.06 to 2.72]; $P=0.029$) and OS (HR, 1.81 [95%CI, 1.07 to 3.08]; $P=0.029$). AFP ≥ 400 ng/mL (HR, 2.06 [95%CI, 1.25 to 3.40]; $P=0.004$) was associated with the reduced OS. More importantly, higher tumor ECV was independent protection factor for longer PFS (HR, 0.47 [95% CI, 0.31 to 0.71]; $P<0.001$) and OS (HR, 0.38 [95%CI, 0.24 to 0.63]; $P<0.001$) (Tables 2 and 3).

Characteristics	Univariate analysis		Multivariate analysis	
	Hazard ratio (95% CI)	P value	Hazard ratio (95% CI)	P value
Age (years)				
< 60	Reference		Reference	
≥ 60	0.719 (0.490–1.055)	0.092	0.716 (0.477–1.077)	0.109
Sex				
Female	Reference			
Male	0.963 (0.566–1.641)	0.891		
BMI(kg/m ²)	0.973 (0.914–1.036)	0.394		
HBV infection				
No	Reference			
Yes	0.872 (0.598–1.272)	0.477		
Types of ICIs				
PD-1	Reference			
PD-L1	0.625 (0.296–1.321)	0.218		
Combined with TKIs				
No	Reference			
Yes	1.182 (0.812–1.722)	0.383		
Tumor maximum diameter (cm)	1.044 (0.999–1.090)	0.054	1.010 (0.961–1.062)	0.691
Tumor number				
≤ 3	Reference			
> 3	1.353 (0.839–2.181)	0.215		
PVTT				
No	Reference		Reference	
Yes	1.692 (1.143–2.504)	0.009	1.247 (0.773–2.013)	0.365
Lymph node metastasis				
No	Reference			
Yes	1.234 (0.808–1.884)	0.331		
BCLC stage				
B	Reference		Reference	
C	1.998 (1.357–2.944)	<0.001	1.694 (1.055–2.719)	0.029
Child-Pugh				
A	Reference			
B	0.987 (0.537–1.813)	0.965		
ECOG PS				
0	Reference			
≥ 1	1.207 (0.782–1.864)	0.396		
NLR	1.088 (1.000–1.183)	0.049	1.091 (0.983–1.211)	0.101
PLR	1.003 (1.001–1.004)	0.005	1.001 (0.999–1.003)	0.385
ALT(U/L)	1.000 (0.999–1.002)	0.648		
AST(U/L)	1.001 (0.999–1.003)	0.289		
TB (μmol/L)	1.004 (0.989–1.019)	0.624		
Albumin (g/L)	0.994 (0.957–1.032)	0.745		
PT (s)	0.932 (0.809–1.074)	0.329		
Urea nitrogen (mmol/L)	0.968 (0.868–1.079)	0.558		
Creatinine (μmol/L)	0.996 (0.985–1.008)	0.512		
AFP (ng/mL)				
< 400	Reference			
≥ 400	1.291 (0.881–1.891)	0.190		
Liver ECV group				
Continued				

Characteristics	Univariate analysis		Multivariate analysis	
	Hazard ratio (95% CI)	P value	Hazard ratio (95% CI)	P value
Lower liver ECV	Reference			
Higher liver ECV	1.198 (0.823–1.744)	0.346		
Tumor ECV group				
Lower tumor ECV	Reference		Reference	
Higher tumor ECV	0.502 (0.340–0.742)	<0.001	0.471 (0.314–0.709)	<0.001

Table 2. Univariate and multivariate Cox proportional hazards analyses for PFS. Significant values are given in bold. PFS progression-free survival, ECV extracellular volume, CI confidence interval, BMI body mass index, HBV hepatitis B virus, ICIs immune checkpoint inhibitors, TKIs tyrosine kinase inhibitors, PVTT portal vein tumor thrombosis, BCLC Barcelona clinic liver cancer, ECOG PS eastern cooperative oncology group physical status, NLR neutrophil to lymphocyte ratio, PLR platelet to lymphocyte ratio, ALT alanine transaminase, AST aspartate transaminase, TB total bilirubin, PT prothrombin time, AFP alpha-fetoprotein.

Subgroup analysis

Subgroup analyses were performed according to baseline characteristics, in which relative consistency in PFS and OS results were observed. In subgroup analysis of PFS in tumor ECV patients, the risk of short PFS was lower in the Higher tumor ECV group than in the Lower tumor ECV group except for the PD-L1 usage and Child-Pugh B subgroups (Supplementary Fig. 3). In the subgroup of tumor number > 3 (HR 0.42 [95% CI, 0.17, 1.06]), ECOG PS \geq 1 (0.49 [95% CI, 0.22, 1.08]) and Lower liver ECV (HR 0.59 [95% CI, 0.33, 1.04]), there was a trend toward longer OS in the Higher tumor ECV group compared to the Lower tumor ECV group, although the difference was not statistically significant. However, in the subgroup analyses of OS (Fig. 5), a lower risk of short OS in the Higher tumor ECV group than in the Lower tumor ECV group was observed in each of the subgroups of age, sex, HBV infection, combined with TKIs, tumor number and lymph node metastasis. We also discovered interactions between sex ($P=0.014$) and the presence of PVTT ($P=0.021$) with tumor ECV fraction. In addition, the liver ECV fraction level had no potential effect on PFS and OS in all the subgroups (Supplementary Fig. 4 and Supplementary Fig. 5).

Repeatability of cutoff values

In the internal validation cohort, patients were grouped using a tumor ECV of 27.2% and a liver ECV of 29.0% as thresholds. There were 27 patients in the lower tumor ECV group and 33 in the higher tumor ECV group, and 33 patients in the lower liver ECV group and 27 in the higher liver ECV group. The median PFS was 8.2 months and the median OS was 12.8 months in the internal validation cohort. The KM curves showed that the high tumor ECV group had longer PFS (10.9 months vs. 5.4 months, $P=0.025$) and OS (14.3 months vs. 11.5 months, $P=0.023$) than the lower tumor ECV group (Supplementary Fig. 6). However, there were no significant differences in PFS (7.7 vs. 8.2 months, $P=0.552$) and OS (11.5 vs. 13.7 months, $P=0.110$) between the Lower liver ECV and Higher liver ECV groups. In multivariate analysis, PT was independent risk factor for PFS (HR, 1.28 [95%CI, 1.08 to 1.52]; $P=0.005$, Supplementary Table 4). The Age \geq 60 years, BCLC-C stage and AFP \geq 400ng/mL were associated with the reduced OS. Furthermore, higher tumor ECV was independent protection factor for longer PFS (HR, 0.32 [95% CI, 0.15 to 0.68]; $P=0.003$) and OS (HR, 0.35 [95%CI, 0.14 to 0.85]; $P=0.020$) (Supplementary Table 5).

Discussion

In this study, we retrospectively analyzed tumor ECV fraction and liver ECV fraction measured using equilibrium CECT before ICIs therapy in HCC patients in order to predict their survival outcomes. Our study showed that tumor ECV fraction showed a significant positive correlation with liver ECV fraction. The Higher tumor ECV group had longer PFS and OS than the Lower tumor ECV group, whereas no similar results were found for the lower and higher liver ECV groups. The tumor ECV fraction was an independent predictor of PFS and OS in patients. Therefore, tumor ECV fraction quantified with equilibrium CECT compared to liver ECV fraction may serve as a novel imaging indicator for HCC patients receiving ICIs, enabling the identification of individuals who may not derive therapeutic benefit from ICIs treatment and contributing to prompt adjustment of their treatment plans.

The effectiveness of tumor treatment can be influenced by the extravascular extracellular volume fraction surrounding tumor tissue²³. CECT provides valuable insight assessing the vascular distribution of many tumors, which can be readily applied in clinical practice. The ECV fraction is a reliable indicator that is not significantly impacted by several technical confounders or physiological variability as well as its easy to calculate²⁴. Research has demonstrated the potential predictive utility of ECV fraction as an imaging marker for many tumors such as pancreatic cancer, cervical squamous cell carcinoma, etc.^{14,23}. Fukukura et al. discovered that CT-derived ECV fraction could independently predict the PFS and OS in patients with PDAC, and ECV fraction also had a high diagnostic value in predicting the survival of patients with stage IV PDAC who received chemotherapy^{23,25}. Similarly, Iwawa et al. demonstrated that CT-derived ECV fraction was a significant prognostic factor of OS in pancreatic cancer patients²⁶.

In the liver, previous studies investigated the relationship between various imaging parameters and HCC histopathologic features, treatment response prediction, and prognosis. Wu et al. developed a prediction model

Characteristics	Univariate analysis		Multivariate analysis	
	Hazard ratio (95% CI)	P value	Hazard ratio (95% CI)	P value
Age (years)				
< 60	Reference			
≥ 60	0.816 (0.519–1.283)	0.378		
Sex				
Female	Reference		Reference	
Male	1.883 (0.899–3.943)	0.093	1.776 (0.820–3.846)	0.145
BMI(kg/m ²)	0.977 (0.906–1.053)	0.538		
HBV infection				
No	Reference			
Yes	0.832 (0.529–1.309)	0.426		
Types of ICIs				
PD-1	Reference			
PD-L1	0.702 (0.303–1.623)	0.407		
Combined with TKIs				
No	Reference			
Yes	1.001 (0.648–1.546)	0.998		
Tumor maximum diameter (cm)	1.085 (1.031–1.142)	0.002	1.027 (0.965–1.093)	0.406
Tumor number				
≤ 3	Reference			
> 3	0.832 (0.478–1.448)	0.516		
PVT				
No	Reference		Reference	
Yes	1.771 (1.142–2.746)	0.011	1.341 (0.826–2.177)	0.236
Lymph node metastasis				
No	Reference			
Yes	1.203 (0.741–1.952)	0.455		
BCLC stage				
B	Reference		Reference	
C	2.348 (1.458–3.782)	< 0.001	1.809 (1.062–3.083)	0.029
Child-Pugh				
A	Reference			
B	1.563 (0.802–3.044)	0.190		
ECOG PS				
0	Reference			
≥ 1	1.358 (0.766–2.408)	0.295		
NLR	1.119 (1.001–1.252)	0.049	1.117 (0.972–1.283)	0.118
PLR	1.002 (1.000–1.004)	0.106		
ALT(U/L)	1.000 (0.999–1.001)	0.849		
AST(U/L)	1.001 (0.999–1.003)	0.299		
TB (μmol/L)	1.004 (0.992–1.016)	0.537		
Albumin (g/L)	0.980 (0.937–1.025)	0.386		
PT (s)	1.059 (0.895–1.254)	0.503		
Urea nitrogen (mmol/L)	0.959 (0.841–1.093)	0.529		
Creatinine (μmol/L)	0.995 (0.982–1.009)	0.486		
AFP (ng/mL)				
< 400	Reference		Reference	
≥ 400	2.562 (1.632–4.023)	< 0.001	2.064 (1.253–3.399)	0.004
Liver ECV group				
Continued				

Characteristics	Univariate analysis		Multivariate analysis	
	Hazard ratio (95% CI)	P value	Hazard ratio (95% CI)	P value
Lower liver ECV	Reference			
Higher liver ECV	1.080 (0.700–1.666)	0.728		
Tumor ECV group				
Lower tumor ECV	Reference		Reference	
Higher tumor ECV	0.382 (0.235–0.621)	<0.001	0.384 (0.235–0.628)	<0.001

Table 3. Univariate and multivariate Cox proportional hazards analyses for OS. Significant values are given in bold. OS overall survival, ECV extracellular volume, CI confidence interval, BMI body mass index, HBV hepatitis B virus, ICIs immune checkpoint inhibitors, TKIs tyrosine kinase inhibitors, PVTT portal vein tumor thrombosis, BCLC Barcelona clinic liver cancer, ECOG PS eastern cooperative oncology group physical status, NLR neutrophil to lymphocyte ratio, PLR platelet to lymphocyte ratio, ALT alanine transaminase, AST aspartate transaminase, TB total bilirubin, PT prothrombin time, AFP alpha-fetoprotein.

based on the radiological features of MRI and clinical factors, which effectively predicted pathological grades of HCC²⁷. The arterial scores of Dynamic contrast-enhanced (DCE)-MRI using the Tofts model were significantly higher in moderately differentiated HCC compared with poorly differentiated HCC²⁸. Malignant tumor cells had higher K^{trans} (contrast agent transfer rate constant from plasma to extravascular extracellular space) and k_{ep} (contrast agent intravasation rate constant) and lower V_e (extravascular extracellular volume fraction) compared to normal liver tissue and benign tumors, where these parameters were derived from DCE-MRI²⁹. As the pathological grading of HCC increases, the tumor cells are disorganized and tightly arranged, the distribution of the contrast agent in the extravascular extracellular space decreased, leading to an increase in K^{trans} , k_{ep} , and a decrease in V_e . Moreover, Kim et al. evaluated magnetic resonance perfusion and diffusion parameters prior to concurrent chemoradiotherapy (CCRT)³⁰. They found that PFS was significantly longer in patients with higher apparent diffusion coefficient values than those with lower values. These previous studies investigated the characteristics of HCC from different dimensions and using various imaging techniques and parameters. And there was evidence that tumor ECV fraction predicted the degree of pathologic differentiation of HCC, most liver ECV fraction studies focused on assessing the severity of liver fibrosis and cirrhosis^{18,19}. These provided a rich research background and reference perspective for the present study on the use of ECV to assess the prognosis of HCC patients treated with ICIs.

To our knowledge, the present study was the first to investigate the association between tumor ECV and liver ECV fraction, as well as to report the relationship of ECV fraction with survival outcomes in HCC patients receiving ICIs. We revealed a positive correlation between tumor ECV and liver ECV, probably due to HCC growth affecting the overall microenvironment of the liver, with tumor-associated angiogenesis and inflammatory responses in the liver contributing to the positive correlation. We also found that OS was longer in the Higher tumor ECV group (15.5 months vs. 10.5 months) than in the Lower tumor ECV group, whereas there were no similar results in the higher and lower liver ECV groups. Tumor ECV fraction was an independent predictor of PFS and OS in HCC patients receiving ICIs therapy. Unraveling the underlying mechanisms of this correlation is a challenging task, various plausible rationales can be considered. Initially, ICIs activate anti-tumor immune responses by deregulating T cell immunosuppression. In contrast to liver ECV fraction, tumor ECV fraction reflects angiogenesis, immune cell infiltration, and tumor cell interactions in the tumor microenvironment, which influence the immunotherapeutic response. In addition, the ECV fraction include both the intravascular space fraction and the extravascular extracellular volume component. Benjaminsen et al.³¹ demonstrated a positive correlation between tumor ECV fraction and tumor extravascular ECV fraction in human melanoma xenografts. Also, the aggressiveness of tumors and the absorption of anticancer drugs are indeed influenced by the extravascular ECV fraction^{32,33}. Likewise, tumor ECV fraction in HCC patients may play an important role in ICIs delivery.

The other possible reason is that ECV is often considered to be associated with factors such as tissue angiogenesis and cell proliferation. Cui et al. found CT-derived ECV values hold promise in evaluating the differentiation grade of HCC³⁴. Specifically, the ECV was notably higher in the well differentiated group compared to the poorly differentiated group. Li et al. also successfully developed and validated a CT-derived ECV-based noninvasive adjunctive assessment method to predict HCC pathological information¹⁸. This is probably due to the fact that ECV refers to the fluid environment surrounding the cells. When this environment is defective, tumor cells may be restricted, resulting in a poorer state of differentiation. This means the tumor cells may become immature or function abnormally. In addition, ECV has an important role in angiogenesis. Tumor cells require angiogenesis to provide sufficient oxygen and nutrients for their growth. If low ECV affects angiogenesis, it could result in an inadequate supply of blood vessels within the tumor, which in turn affects the growth and differentiation status of the tumor. Inadequate ECV may also prevent tumor cells from obtaining sufficient oxygen and nutrients and therefore possibly show a poorer degree of differentiation. Based on the above theories, the poor prognosis of patients with low ECV fraction in this study could be attributed to the lower differentiation of HCC in these patients. In addition, the higher tumor ECV group had a higher proportion of BCLC-B stage compared to the lower tumor ECV group at present study, despite the lack of statistical significance. Therefore, the lower BCLC stage, the better pathologic differentiation of HCC¹⁸, which probably responds better to treatment leading to a better prognosis after treatment with ICIs.

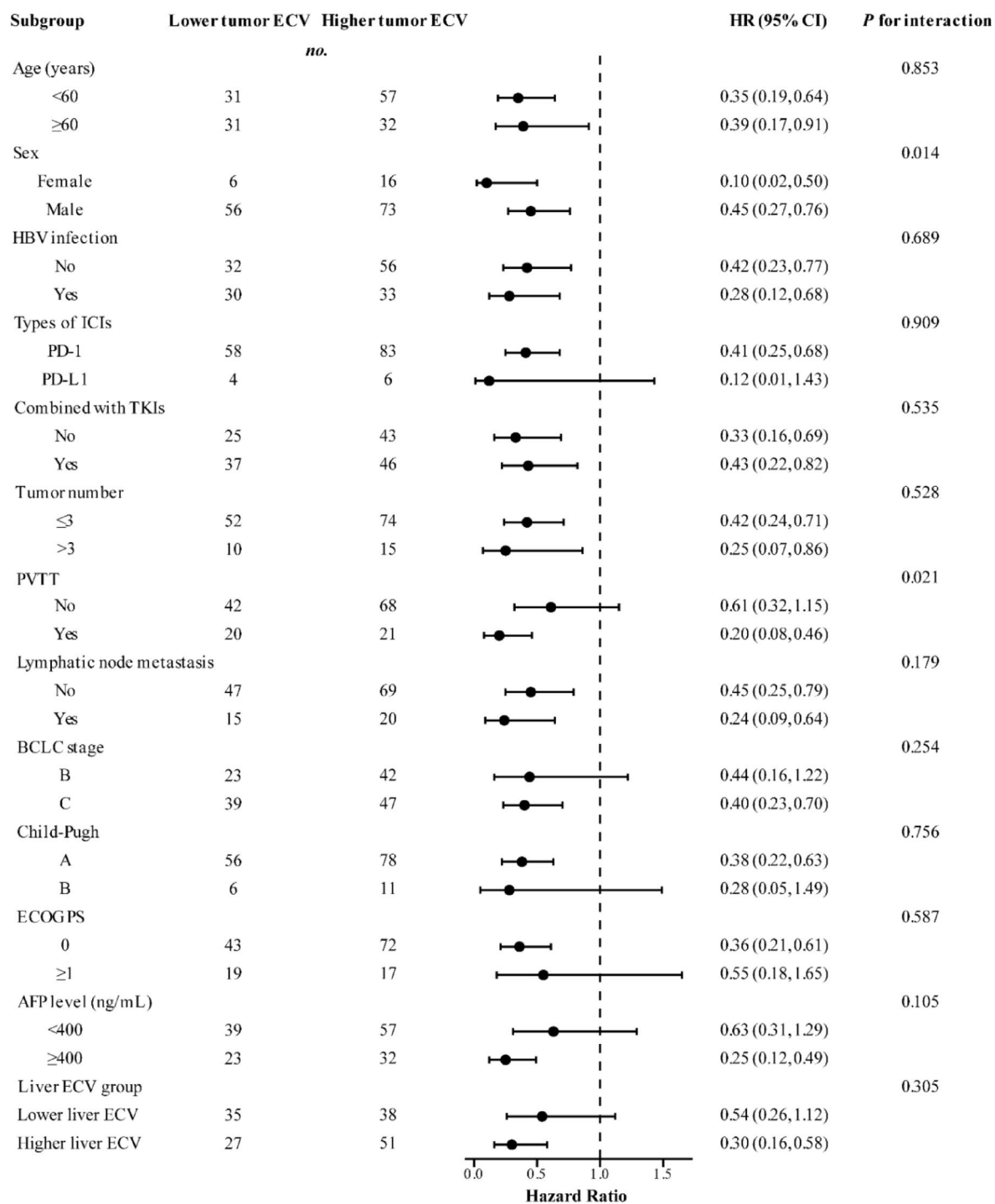


Fig. 5. Forest plot of subgroup analysis of overall survival between Lower tumor ECV and Higher tumor ECV groups. The dashed line indicates a risk ratio of 1. *ECV* extracellular volume, *HBV* hepatitis B virus, *ICIs* immune checkpoint inhibitors, *TKIs* tyrosine kinase inhibitors, *PVTT* portal vein tumor thrombosis, *BCLC stage* Barcelona clinic liver cancer stage, *ECOG PS* eastern cooperative oncology group physical status, *AFP* alpha-fetoprotein.

Numerous clinical and laboratory markers can be used to forecast survival outcomes in HCC patients receiving ICIs therapy^{35–37}. AFP, which is produced by the fetal liver, should normally be present in low levels in healthy adults. The predictive ability of AFP in determining the prognosis of patients with HCC has been validated³⁶. Our study found that AFP ≥ 400 ng/ml was an independent risk factor for OS in HCC patients receiving ICIs, which is similar to previous studies^{35,38}. The IMbrave 150 study discovered that immunotherapy prolonged survival with serum AFP levels < 400 ng/mL in unresectable HCC patients³⁸. And the AFP reduction > 50% was positively associated with longer OS in the HCC patients receiving PD-1³⁶. This phenomenon can be attributed

to malignant cancer cells that develop from hepatocytes possibly lead to re-expression of AFP³⁹, of which high levels tend to indicate higher tumor burden, greater aggressiveness and poorer liver function, leading ultimately to poorer survival. Another important clinical indicator is BCLC stage, the basis for clinical treatment of HCC⁴⁰. Recent phase III studies on HCC immunotherapy have focused on HCC patients with BCLC-B and BCLC-C^{41–43}. In general, the BCLC staging system is usually used to assess the progression and prognosis of HCC⁴⁰. The higher BCLC stage, the shorter survival time of patients receiving ICIs for HCC patients, which was confirmed in our study. We demonstrated that BCLC-C stage was an independent risk factor for shorter PFS and OS in patients with HCC patients receiving ICIs, probably owing to the fact that the higher the BCLC grading, the worse the liver function and patient performance status, and consequently, the poorer the response to treatment.

This study still has some limitations. Firstly, this study is a single-center retrospective study that may have selection bias. Although we performed a simple internal validation, the generalizability of the findings is still limited. Therefore, future prospective external multicenter clinical trials are necessary to validate our findings. Second, the hematocrit for calculating ECV fraction was not obtained with CT on the same day, it is possible for fluctuations in hematocrit in some patients, but we have controlled the time interval between the measured hematocrit and the CT scan to be less than one week. Third, the accuracy of ECV fraction is affected by the choice of equilibrium CECT time. Currently, it is lacking a known optimal balancing time to obtain high-quality equilibration images. Yoon et al.⁴⁴ reported that the 3-minute equilibration to assess the ECV fraction is suitable balance between clinical workflow and technical success. In addition, a study used the equilibration CECT of 120–150 s to evaluate the ECV fraction of HCC patients¹⁸. In conjunction with prior research, we used 120–180 s of equilibrium CECT to ensure image quality as much as possible. However, the ideal equilibrium phase timing for ECV measurement (120–180 s vs. >3 min) remains uncertain. Therefore, we need to standardize imaging protocols in future studies for better reproducibility.

Conclusions

In this study, we showed that a positive correlation between tumor ECV fraction and liver ECV fraction. Tumor ECV fraction measured by equilibrium CECT in HCC patients undergoing ICIs therapy predicts survival compared to liver ECV fraction, which consequently may be helpful for their monitoring and management.

Data availability

The datasets used and/or analyzed in this study are available from the corresponding author on reasonable request.

Received: 6 January 2025; Accepted: 7 April 2025

Published online: 20 April 2025

References

- Sangro, B., Sarobe, P., Hervas-Stubbs, S. & Melero I. Advances in immunotherapy for hepatocellular carcinoma. *Nat. Rev. Gastroenterol. Hepatol.* **18**, 525–543 (2021).
- Sung, H. et al. Global cancer statistics 2020: GLOBOCAN estimates of incidence and mortality worldwide for 36 cancers in 185 countries. *CA Cancer J. Clin.* **71**, 209–249 (2021).
- Wang, W. & Wei, C. Advances in the early diagnosis of hepatocellular carcinoma. *Genes Dis.* **7**, 308–319 (2020).
- Foerster, F., Gairing, S. J., Ilyas, S. I. & Galle, P. R. Emerging immunotherapy for HCC: A guide for hepatologists. *Hepatology* **75**, 1604–1626 (2022).
- Cheng, A. L., Hsu, C., Chan, S. L., Choo, S. P. & Kudo, M. Challenges of combination therapy with immune checkpoint inhibitors for hepatocellular carcinoma. *J. Hepatol.* **72**, 307–319 (2020).
- Peters, S., Kerr, K. M. & Stahel, R. PD-1 Blockade in advanced NSCLC: A focus on pembrolizumab. *Cancer Treat. Rev.* **62**, 39–49 (2018).
- Deutsch, J. S. et al. Combinatorial biomarker for predicting outcomes to anti-PD-1 therapy in patients with metastatic clear cell renal cell carcinoma. *Cell. Rep. Med.* **4**, 100947 (2023).
- Pinter, M., Jain, R. K. & Duda, D. G. The current landscape of immune checkpoint Blockade in hepatocellular carcinoma: A review. *JAMA Oncol.* **7**, 113–123 (2021).
- Gao, R. et al. Deep learning for differential diagnosis of malignant hepatic tumors based on multi-phase contrast-enhanced CT and clinical data. *J. Hematol. Oncol.* **14**, 154 (2021).
- Karamanos, N. K. et al. A guide to the composition and functions of the extracellular matrix. *Febs J.* **288**, 6850–6912 (2021).
- Liu, Y. et al. Identification of a tumour immune barrier in the HCC microenvironment that determines the efficacy of immunotherapy. *J. Hepatol.* **78**, 770–782 (2023).
- Adams, L. C. et al. Assessment of the extracellular volume fraction for the grading of clear cell renal cell carcinoma: first results and histopathological findings. *Eur. Radiol.* **29**, 5832–5843 (2019).
- Peng, Y. et al. Nomogram based on CT-derived extracellular volume for the prediction of post-hepatectomy liver failure in patients with resectable hepatocellular carcinoma. *Eur. Radiol.* **32**, 8529–8539 (2022).
- Li, S. et al. T1 mapping and extracellular volume fraction measurement to evaluate the poor-prognosis factors in patients with cervical squamous cell carcinoma. *NMR Biomed.* **36**, e4918 (2023).
- Takumi, K. et al. Extracellular volume fraction derived from equilibrium contrast-enhanced CT as a diagnostic parameter in anterior mediastinal tumors. *Eur. J. Radiol.* **165**, 110891 (2023).
- Fukukura, Y. et al. Estimation of extracellular volume fraction with routine multiphase pancreatic computed tomography to predict the survival of patients with stage IV pancreatic ductal adenocarcinoma. *Pancreas* **48**, 1360–1366 (2019).
- Luo, Y. et al. Extracellular volume fraction determined by equilibrium contrast-enhanced CT for the prediction of the pathological complete response to neoadjuvant chemoradiotherapy for locally advanced rectal cancer. *Eur. Radiol.* **33**, 4042–4051 (2023).
- Li, J. et al. Interpretable machine learning based on CT-derived extracellular volume fraction to predict pathological grading of hepatocellular carcinoma. *Abdom. Radiol. (NY)*. **49**, 3383–3396 (2024).
- Bandula, S. et al. Equilibrium contrast-enhanced CT imaging to evaluate hepatic fibrosis: initial validation by comparison with histopathologic sampling. *Radiology* **275**, 136–143 (2015).
- von Elm, E. et al. The strengthening of reporting of observational studies in epidemiology (STROBE) statement: guidelines for reporting observational studies. *Lancet* **370**, 1453–1457 (2007).

21. Liver, E. A. et al. EASL clinical practice guidelines: management of hepatocellular carcinoma. *J. Hepatol.* **69**, 182–236 (2018).
22. Lencioni, R., Llovet, J. M. & Modified RECIST (mRECIST) assessment for hepatocellular carcinoma. *Semin. Liver Dis.* **30**, 52–60 (2010).
23. Fukukura, Y. et al. Extracellular volume fraction determined by equilibrium contrast-enhanced multidetector computed tomography as a prognostic factor in unresectable pancreatic adenocarcinoma treated with chemotherapy. *Eur. Radiol.* **29**, 353–361 (2019).
24. Kim, P. K. et al. Myocardial extracellular volume fraction and change in hematocrit level: MR evaluation by using T1 mapping in an experimental model of anemia. *Radiology* **288**, 93–98 (2018).
25. Fukukura, Y. et al. Extracellular volume fraction determined by equilibrium contrast-enhanced dual-energy CT as a prognostic factor in patients with stage IV pancreatic ductal adenocarcinoma. *Eur. Radiol.* **30**, 1679–1689 (2020).
26. Iwaya, H. et al. Prognostic significance of extracellular volume fraction with equilibrium contrast-enhanced computed tomography for pancreatic neuroendocrine neoplasms. *Pancreatol.* **21**, 779–786 (2021).
27. Wu, M. et al. Predicting the grade of hepatocellular carcinoma based on non-contrast-enhanced MRI radiomics signature. *Eur. Radiol.* **29**, 2802–2811 (2019).
28. Jajamovich, G. H. et al. DCE-MRI of hepatocellular carcinoma: perfusion quantification with Tofts model versus shutter-speed model—initial experience. *Magma* **29**, 49–58 (2016).
29. Song, Q. et al. Study of microcirculation function status of HCC using 3D-DCE-MRI perfusion Tofts model. *Radiol. Pract.* **28**, 662–665 (2013).
30. Kim, K. A. et al. Diffusion and perfusion MRI prediction of progression-free survival in patients with hepatocellular carcinoma treated with concurrent chemoradiotherapy. *J. Magn. Reson. Imaging.* **39**, 286–292 (2014).
31. Benjaminsen, I. C., Brurberg, K. G., Ruud, E. B. & Rofstad, E. K. Assessment of extravascular extracellular space fraction in human melanoma xenografts by DCE-MRI and kinetic modeling. *Magn. Reson. Imaging.* **26**, 160–170 (2008).
32. Krol, A., Maresca, J., Dewhirst, M. W. & Yuan, F. Available volume fraction of macromolecules in the extravascular space of a fibrosarcoma: implications for drug delivery. *Cancer Res.* **59**, 4136–4141 (1999).
33. Jain, R. K. Transport of molecules in the tumor interstitium: a review. *Cancer Res.* **47**, 3039–3051 (1987).
34. Cui, F. et al. Exploration of evaluating the differentiation degree of hepatocellular carcinoma by using extracellular volume fraction. *Oncoradiology* **29**, 303–307 (2020).
35. Zhang, N. et al. Biomarkers and prognostic factors of PD-1/PD-L1 inhibitor-based therapy in patients with advanced hepatocellular carcinoma. *Biomark. Res.* **12**, 26 (2024).
36. Sun, X. et al. Reductions in AFP and PIVKA-II can predict the efficiency of anti-PD-1 immunotherapy in HCC patients. *BMC Cancer.* **21**, 775 (2021).
37. Muller, L. et al. Portal hypertension in patients with hepatocellular carcinoma and immunotherapy: prognostic relevance of CT-morphologic estimates. *Cancer Imaging.* **23**, 40 (2023).
38. Finn, R. S. et al. Atezolizumab plus bevacizumab in unresectable hepatocellular carcinoma. *N. Engl. J. Med.* **382**, 1894–1905 (2020).
39. Woo, H. Y. et al. Lung and lymph node metastases from hepatocellular carcinoma: comparison of pathological aspects. *Liver Int.* **42**, 199–209 (2022).
40. Reig, M. et al. BCLC strategy for prognosis prediction and treatment recommendation: the 2022 update. *J. Hepatol.* **76**, 681–693 (2022).
41. Kelley, R. K. et al. VP10-2021: Cabozantinib (C) plus Atezolizumab (A) versus Sorafenib (S) as first-line systemic treatment for advanced hepatocellular carcinoma (aHCC): results from the randomized phase III COSMIC-312 trial. *Ann. Oncol.* **33**, 114–116 (2022).
42. Ren, Z. et al. Sintilimab plus a bevacizumab biosimilar (IBI305) versus Sorafenib in unresectable hepatocellular carcinoma (ORIENT-32): a randomised, open-label, phase 2–3 study. *Lancet Oncol.* **22**, 977–990 (2021).
43. Llovet, J. M. et al. Lenvatinib (len) plus pembrolizumab (pembro) for the first-line treatment of patients (pts) with advanced hepatocellular carcinoma (HCC): phase 3 LEAP-002 study. *J. Clin. Oncol.* **37**, TPS4152–TPS4152 (2019).
44. Yoon, J. H. et al. Estimation of hepatic extracellular volume fraction using multiphasic liver computed tomography for hepatic fibrosis grading. *Invest. Radiol.* **50**, 290–196 (2015).

Acknowledgements

We would like to thank all the investigators and patients.

Author contributions

XNF: visualization, writing the original draft, review, and editing. YSG: funding acquisition, writing the original draft, review, and editing. KLZ: data curation, writing the original draft, review, and editing. ZXC: data curation, visualization. CYL: investigation, visualization. YR, WWL: formal analysis. LWM: data curation. SSJ: project administration. CZ: investigation, supervision, review and editing. YBS: visualization, supervision, review, and editing. LY: funding acquisition, supervision, review, and editing.

Funding

The author(s) declared financial support was received for the research, authorship, and/or publication of this article. This study was supported by grants from National Key Research and Development Program of China (2023YFE0113300), the Major Special Project for Technology Innovation of Hubei Province (2023BCB014), National Natural Science Foundation of China (82172034) and the Fundamental Research Funds for the Central Universities (20242422).

Declarations

Competing interests

The authors declare no competing interests.

Ethics statement

The study was approved by the Research Ethics Committee of Tongji Medical College, Huazhong University of Science and Technology (Institutional Review Board No. S049). Due to the retrospective and anonymous analysis of the clinical data, the Ethics Committee of Tongji Medical College waived the requirement for written informed consent from participants or their legal guardians/next of kin.

Additional information

Supplementary Information The online version contains supplementary material available at <https://doi.org/10.1038/s41598-025-97677-x>.

Correspondence and requests for materials should be addressed to C.Z., Y.S. or L.Y.

Reprints and permissions information is available at www.nature.com/reprints.

Publisher's note Springer Nature remains neutral with regard to jurisdictional claims in published maps and institutional affiliations.

Open Access This article is licensed under a Creative Commons Attribution-NonCommercial-NoDerivatives 4.0 International License, which permits any non-commercial use, sharing, distribution and reproduction in any medium or format, as long as you give appropriate credit to the original author(s) and the source, provide a link to the Creative Commons licence, and indicate if you modified the licensed material. You do not have permission under this licence to share adapted material derived from this article or parts of it. The images or other third party material in this article are included in the article's Creative Commons licence, unless indicated otherwise in a credit line to the material. If material is not included in the article's Creative Commons licence and your intended use is not permitted by statutory regulation or exceeds the permitted use, you will need to obtain permission directly from the copyright holder. To view a copy of this licence, visit <http://creativecommons.org/licenses/by-nc-nd/4.0/>.

© The Author(s) 2025